Regular Article

PHYSICAL CHEMISTRY RESEARCH
Published by the
Iranian Chemical Society
www.physchemres.org
info@physchemres.org

Phys. Chem. Res., Vol. 11, No. 3, 511-525, September 2023
DOI: 10.22036/pcr.2022.341501.2098

Reactivity of Isothiasole with Dibromine and Sulfuryl Chloride

Z. Jalil[a], El H. El Karni[a], T. EL Ouafy[b], M. Echajia[a], M. Mbarki[a] and M. Oubenali[a,*]

[a]*Laboratory of Engineering in Chemistry and Physics of Matter, Department of Chemistry and Environment, Faculty of Science and Technics, Sultan Moulay Slimane University, Beni Mellal, Morocco*

[b]*Laboratory of Engineering in Chemistry and Physics of Matter, Department of Physics and Chemistry, Polydisciplinary Faculty of Khouribga, Sultan Moulay Slimane University, Beni Mellal, Morocco*

(Received 2 June 2022, Accepted 25 July 2022)

In this work, we studied the reactivity of the 4-isothiazolin-3-one and 2-methyl-4-isothiazolin-3-one molecules with dibromine and sulfuryl chloride using the DFT method with 6-311G(d,p) basis set and a descriptor of regio-selectivity called Fukui indices. The results showed that the attack of dibromine and sulfuryl chloride occurred preferentially at the C_2=C_3 bond of 4-isothiazoline-3-one and 2-methyl-4-isothiazoline-3-one. In addition, the 4-isothiazolin-3-one/SO_2Cl_2 and 2-methyl-4-isothiazolin-3-one/SO_2Cl_2 reactions were more kinetically favorable than the 4-isothiazolin-3-one/Br_2 and 2-methyl- 4-isothiazolin-3-one/Br_2 reactions. The differences in electrophilic index ($\Delta\omega$) of {Br_2, SO_2Cl_2} and 4-isothiazolin-3-one, or {Br_2, SO_2Cl_2} and 2-methyl-4-isothiazolin-3-one were from 3.430649 eV to 3.611297 eV. This shows that all the studied reactions had a polar character ($\Delta\omega > 1$).

Keywords: DFT, Chemical descriptor, 2-Methyl-4-isothiazoline-3-one, 4-Isothiazolin-3-one, Dibromine, Sulfuryl chloride

INTRODUCTION

Heterocyclic compounds are widely used in new agrochemical research and development [1-5]. Isothiazolinones are heterocyclic compounds characterized by an aromatic nitrogen and sulfur ring, with structural similarities and differences among isothiazolinone derivatives [6].

Until 1990s, isothiazole derivatives such as methylisothiazolinone (MI) was only used as a preservative in cosmetics, at a concentration of 15 ppm in Europe, with a contact sensitization rate of around 2% with a stable trend. After 2000s, MI was introduced as a preservative in non-cosmetic chemicals like paint, inks, lacquers, varnishes, and coolant [7,8].

In dermatology, the frequency of sensitization to MI was constantly around 2.1% from 1998 to 2009. Then, it increased to 3.9% in 2011, in parallel with an increase in the frequency of allergic reactions to MI in the series of preservatives from 1.9% in 2009 to 4.4% in 2011. MI is increasingly used as a preservative in skin care products in recent years [9]. Research showed that MI was an effective antifungal agent against infectious members of the genus Saprolegnia [10].

The aim of our work is to study the reactivity of 4-isothiazolin-3-one and 2-methyl-4-isothiazolin-3-one with dibromine and sulfuryl chloride (Fig. 1) using a descriptor of the local reactivity such as fukui indices.

First, we calculated the global reactivity parameters to predict the electrophilic/nucleophilic character of each molecule. To evaluate the most reactive sites for each molecule, we used molecular electrostatic potential as well as local reactivity parameters using two local reactivity calculation methods such as Hirshfeld indices and Merz-Kollman indices.

The redistribution of electron density (ED) in various bonding and antibonding orbitals and $E_{(2)}$ energies were

*Corresponding author. E-mail: mustapha.oubenali@gmail.com

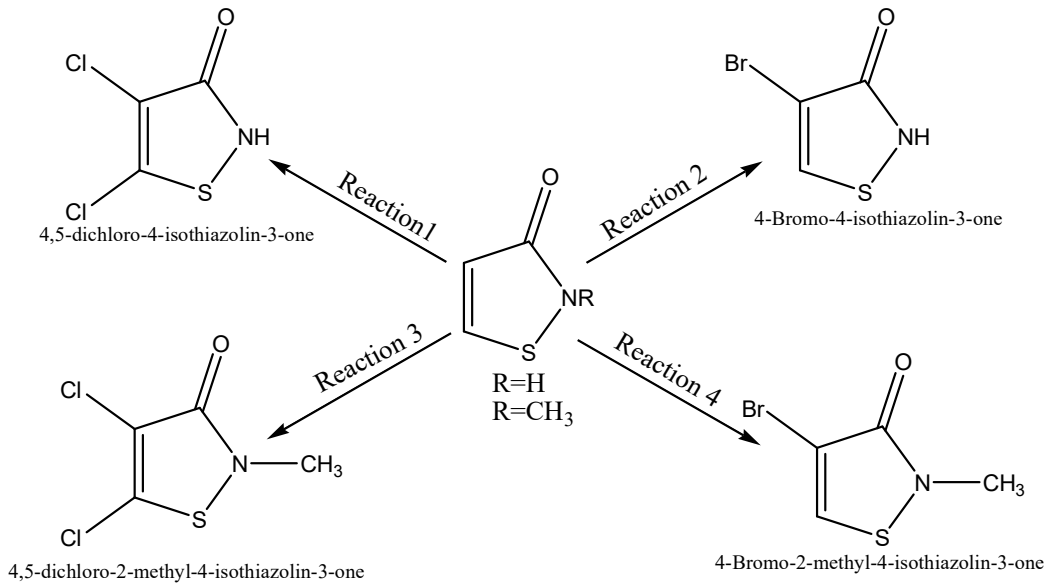

Fig. 1. Geometric structures of the studied molecules.

calculated using of natural bond orbitals (NBO) analysis and DFT method. This gave clear evidence of stabilization from hyper conjugation of various intra-molecular interactions.

The calculation of the maximum absorption wavelengths and the NMR spectra for each molecule were carried out and compared with the experimental results obtained by Lewis *et al.* [11].

Quantum calculations were performed using Gaussian 09W software [12], which is recognized for its advanced capabilities in electronic modeling of chemical structures. The DFT method was chosen, which is the most relevant method in quantum chemistry and allows the study of the electronic structure in an exact way. The 6-311G(d,p) basis set [13,14] was used, which gives more precise results.

CALCULATION METHODS

Quantum chemistry is an indispensable tool for experimentation. It has become a very useful tool in the study and understanding of the stereo-selectivity of concerted reactions. Quantum methods are used to solve the problems of chemical structures and their reactivity. Among the commonly used methods in quantum computing, we selected the DFT method. This method provides important information on the stability of the molecular structure and reactivity [15-19].

In order to highlight the electrophilic and nucleophilic character of the molecules, we calculated the chemical electron potential and global hardness.

The chemical potential (μ) is the negative electronegativity (χ) and is the derivative of total energy relative to the number of electrons (N) at constant external potential, and is given by the below equation [20]:

$$\mu = \frac{E_{HOMO} + E_{LUMO}}{2}$$

Where I and A are the ionization potential and electronic affinity, and E_{HOMO} and E_{LUMO} are the molecular orbital energies of the boundary.

The hardness (η) is the corresponding second derivative defined as follows [21]:

$$\eta = E_{LUMO} - E_{HOMO}$$

The electrophilic index is defined by Parr *et al.* [22-25] as energy decreased due to the maximum electron flow between a donor and an acceptor. They defined the electrophilic index as follows:

$$\omega = \frac{\mu^2}{2\eta}$$

In addition, the maximum number of electrons that an electrophilic compound may acquire is given by the below expression [22,26]:

$$\Delta N_{max} = \frac{-\mu}{\eta}$$

According to Domingo *et al.* [27-29], the global index of nucleophilia, N, is defined by the following formula:

$$N = E_{HOMO(Nu)} - E_{HOMO(TCE)}$$

Here, $E_{HOMO(Nu)}$ is the HOMO energy within the Kohn-Sham scheme [30-32] and $E_{HOMO(TCE)}$ is the HOMO energy of (TCE) which is taken as a reference with the value of -9.3686 eV.

Local electrophilia (ω^+) and local nucleophilia (N^-) at the atomic site k can be defined according to the condensed functions of Fukui, f^+ and f^-.

$$\omega^+ = \omega \times f^+$$

$$N^- = N \times f^-$$

The condensed Fukui functions at the atomic site, for the nucleophilic attack (f^+) and for the electrophilic attack (f^-), can be written in terms of the respective population q(N) of the N-electronic system of the atomic site [33,34].

$$f_k^+ = q_k(N+1) - q_k(N)$$

$$f_k^- = q_k(N) - q_k(N-1)$$

RESULTS AND DISCUSSIONS

Geometry and Optimized Structures of the Studied Molecules

The geometries of the optimized structures, obtained using the DFT method, are shown in Fig. 2.

Prediction of Electrophilic/nucleophilic Character of Reagents

The calculated values of the global reactivity indices, namely the electronic chemical potential μ, the global hardness η, the global electrophilicity, the global

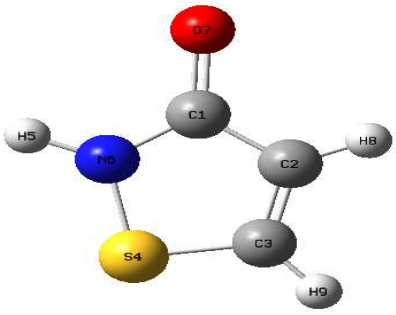

4-Isothiazolin-3-one

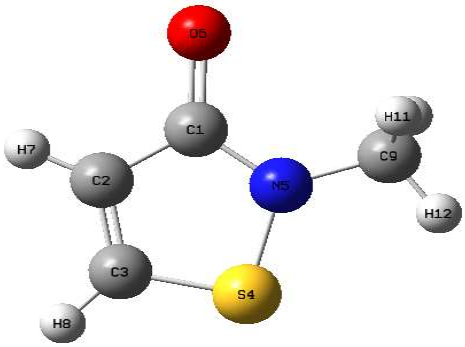

2-Methyl-4-isothiazolin-3-one

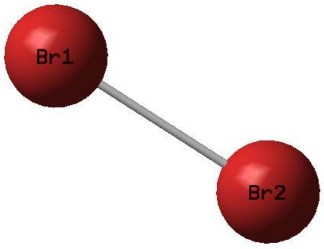

Br_2

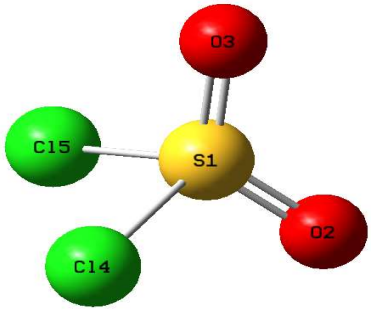

SO_2Cl_2

Fig. 2. Optimized structures of the studied molecules.

nucleophilicity N, the softness, the gap energy, and the electronic affinity for the four molecules are shown in Table 1.

In the case of reaction (1) between 4-isothiazolin-3-one and Br_2 and SO_2Cl_2, the electronic chemical potential of 4-isothiazolin-3-one (μ = -3.74884 eV) was greater than that of Br_2 (μ = -6.06356 eV) and SO_2Cl_2 (μ = -4.4435878 eV); this indicates that the transfer of electrons took place from 4-isothiazolin-3-one toward Br_2 and SO_2Cl_2. On the other hand, the overall electrophilic index of 4-isothiazolin-3-one (ω = 1.370150 eV) was lower than that of the reagents SO_2Cl_2 (ω = 4.720791 eV) and Br_2 (ω = 4.901439 eV); therefore, the Br_2 and SO_2Cl_2 reactants behave as an electrophile, while 4-isothiazolin-3-one behaves as a nucleophile. The same result was obtained for reaction (2) between 2-methyl-4-isothiazolin-3-one and the Br_2 and SO_2Cl_2 reagents.

Moreover, ΔN_{max}, which represents the maximum charge ratio that can be acquired by a system from its environment, was maximum for Br_2 (1.61668 eV) and SO_2Cl_2 (1.32362 eV), and it was minimum for the 4-isothiazolin-3-one (0.73097 eV) and 2-methyl-4-isothiazolin-3-one (0.71495 eV).

In order to show the donor (nucleophilic) or acceptor (electrophilic) character of the reagents and the polar character of the reactions, we calculated the HOMO/LUMO energy differences of the reagents and the differences in electrophilicity (Table 2).

The calculated values of the electrophilic differences varied from 3.430649 eV to 3.611297 eV, showing that all the studied reactions had a polar character, because ($\Delta\omega > 1$) is greater than 1 (Table 2) [35].

The energy difference corresponding to the HOMO(SO_2Cl_2)/LUMO(4-isothiazolin-3-one) combination was greater than that corresponding to the HOMO(4-isothiazolin-3-one)/LUMO(SO_2Cl_2), which shows that 4-isothiazolin-3-one behaves as an acceptor and SO_2Cl_2 as a donor, similar to the results for the other reactions.

Prediction of the Local Reactivity of Reagents

The indices of local electrophilicity and local nucleophilicity are the best descriptors for the prediction of the reactivity and regioselectivity of molecules for formation of a chemical bond. It takes place between the most electrophilic site (characterized by the greatest value of w^+)

Table 1. Electronic Properties of the Studied Molecules

Molecule	HOMO (eV)	LUMO (eV)	μ (eV)	η (eV)	ω (eV)	E_{gap} (eV)	N (eV)	ΔN_{max}
4-Isothiazolin-3-one	-6.31312	-1.18456	-3.74884	5.12856	1.370150	5.12856	3.055448	0.73097
2-methyl-4-isothiazolin-3-one	-6.134416	-1.083648	-3.609032	5.047936	1.290142	5.047936	3.234184	0.71495
SO_2Cl_2	-9.832693	-4.4435878	-7.133140	5.389105	4.720791	5.389105	-0.464093	1.32362
Br_2	-7.938864	-4.188256	-6.06356	3.750608	4.901439	3.750608	1.429736	1.61668

Table 2. Difference between the Two Possible Combinations HOMO/LUMO and $\Delta\omega$

Reaction	Reagent		$\left\lvert E_{HOMO}^{SO_2Cl_2/Br_2} - E_{LUMO}^{molécule} \right\rvert$	$\left\lvert E_{HOMO}^{molécule} - E_{LUMO}^{SO_2Cl_2/Br_2} \right\rvert$	$\Delta\omega$ (eV)
1	4-Isothiazolin-3-one	SO_2CL_2	8.648133	1.8695322	3.35776
2		Br_2	6.754304	2.124864	3.531589
3	2-Methyl-4-isothiazolin-3-one	SO_2CL_2	8.749045	1.6908282	3.430649
4		Br_2	6.855216	1.94616	3.611297

of the electrophilic molecule and the most nucleophilic site (characterized by the greatest value of N^-) of the nucleophilic molecule.

The values of local electrophilicity and local nucleophilicity of the atoms of the 4-isothiazolin-3-one, 2-methyl-4-isothiazolin-3-one, SO_2Cl_2, and Br_2 calculated with the indices of Fukui are given in the Tables 3 and 4.

Tables 3 and 4 show the local nucleophilicity indices (N^-)

Table 3. Local Electrophilic and Nucleophilic Power of the Atoms of 4-Isothiazolin-3-one and SO_2Cl_2, and Br_2 Obtained by a Calculation of the Fukui Indices

Molecule	Atom	Hirshfeld index				Kollman index			
		f^+	f^-	w^+	N^-	f^+	f^-	w^+	N^-
4-Isothiazolin-3-one	1 C	0.06172	0.086474	0.111575	0.225598	0.237157	0.233396	0.324941	0.713129
	2 C	0.151696	0.204492	0.274231	0.53349	0.233423	0.248979	0.319825	0.760742
	3 C	0.108218	0.248399	0.195633	0.648037	0.219682	0.268655	0.300997	0.820861
	4 S	0.337522	0.231683	0.61016	0.604428	0.26892	0.222665	0.368461	0.680341
	6 N	0.137372	0.106816	0.248336	0.278668	0.252237	0.224848	0.345603	0.687011
	7 O	0.203459	0.12213	0.367806	0.31862	0.265618	0.222111	0.363937	0.678649
SO_2CL_2	1 S	0.05641	0.146526	0.303999	-0.068	0.22153	0.295447	1.045797	-0.13711
	2 O	0.107688	0.118769	0.580342	-0.05512	0.224774	0.234253	1.061111	-0.10872
	3 O	0.107688	0.118769	0.580342	-0.05512	0.224774	0.234253	1.061111	-0.10872
	4 Cl	0.364107	0.307971	1.962211	-0.14293	0.275103	0.254409	1.298704	-0.11807
	5 Cl	0.364107	0.307971	1.962211	-0.14293	0.275103	0.254409	1.298704	-0.11807
Br_2	1 Br	0.500003	0.500003	2.450734	0.714872	0.301953	0.285816	1.480004	0.408641

Table 4. Local Electrophilic and Nucleophilic Power of the Atoms of 2-Methyl-4-isothiazolin-3-one and SO_2Cl_2, and Br_2 Obtained by a Calculation of the Fukui Indices

Molecule	Atom	Hirshfeld index				Kollman index			
		f^+	f^-	w^+	N^-	f^+	f^-	w^+	N^-
2-Methyl-4-isothiazolin-3-one	1 C	0.058017	0.079514	0.07485	0.257163	0.230388	0.225347	0.297233	0.728813
	2 C	0.132404	0.197816	0.17082	0.639773	0.220456	0.241968	0.284419	0.782569
	3 C	0.099561	0.240609	0.128448	0.778174	0.208116	0.261071	0.268499	0.844351
	4 S	0.297543	0.212599	0.383873	0.687584	0.252796	0.2152	0.326142	0.69599
	5 N	0.085356	0.042819	0.110121	0.138485	0.249675	0.216317	0.32211	0.699608
	6 O	0.196525	0.112255	0.253545	0.363053	0.260407	0.215128	0.335962	0.695763
	9 C	0.130569	0.114339	0.168453	0.369793	0.183936	0.164391	0.237303	0.531670
SO_2CL_2	1 S	0.05641	0.146526	0.303999	-0.068	0.22153	0.295447	1.045797	-0.13711
	2 O	0.107688	0.118769	0.580342	-0.05512	0.224774	0.234253	1.061111	-0.10872
	3 O	0.107688	0.118769	0.580342	-0.05512	0.224774	0.234253	1.061111	-0.10872
	4 Cl	0.364107	0.307971	1.962211	-0.14293	0.275103	0.254409	1.298704	-0.11807
	5 Cl	0.364107	0.307971	1.962211	-0.14293	0.275103	0.254409	1.298704	-0.11807
Br_2	1 Br	0.500003	0.500003	2.450734	0.714872	0.301953	0.285816	1.480004	0.408641

for the reactive atoms of the 4-isothiazolin-3-one and 2-methyl-4-isothiazolin-3-one molecules, respectively. They also show the local electrophilicity indices (w^+) for the reactive atoms of SO_2Cl_2 and Br_2 calculated by the Fukui indices using DFT.

In the case of reaction between the 4-isothiazolin-3-one and SO_2Cl_2, the most favored interaction took place between the C_2 and C_3 atoms of 4-isothiazolin-3-one (having the highest value of N^-) and the two Cl_4 and Cl_5 atoms of SO_2Cl_2 (with the highest value of w^+). For the case of the reaction between 4-isothiazolin-3-one and Br_2, the most favored interaction took place between the C_3 atoms of 4-isothiazolin-3-one and the Br atom of Br_2 (with the highest value of w^+, Table 3).

Table 4 shows that for the reaction 3, the most favored interaction occurred between the C_2 and C_3 atoms of 2-methyl-4-isothiazolin-3-one and Cl_4 and Cl_5 of SO_2Cl_2, and between the C_3 atom of 2-methyl-4-isothiazolin-3-one and the Br atom of the Br_2 molecule.

The formation of the C_3-Cl, C_2-Cl and C_3-Br bonds of the four reactions has been observed experimentally [11].

Molecular Electrostatic Potential

Molecular electrostatic potential (MEP) gives detailed information for studying the chemical reactivity and biological activity of a compound. The spatial distribution and values of electrostatic potential determine the attack of an electrophile or a nucleophile site as a primary event of a chemical reaction. Moreover, the three-dimensional distribution of electrostatic potential is largely responsible for the binding of a substrate to the active site of a receptor [36]. Molecular electrostatic potential (MEP) is primarily used as a reactivity map, showing the zones most susceptible to electrophilic attack from charged point reactants on organic molecules. This is very important in molecular modeling studies. The MEP contour provides a map that offers a simple tool to predict how different geometries may interact.

The total electron density and the MEP surface of the studied molecules were examined using B3LYP/6-311G(d,p) method. The electrostatic potential maps and the contour electrostatic potential of Br_2, SO_2Cl_2, 4-isothiazolin-3-one, and 2-methyl-4-isothiazolin-3-one are shown in Fig. 3.

The values of the electrostatic potential at the MESP surface are represented by different colors (Fig. 3); red represents zones with the most electronegative electrostatic potential; rich in electrons (partially negative charge), blue represents the zones with the most positive electrostatic potential (zone slightly deficient in electrons), and the green represents the zones with zero potential [37].

From the analysis of Fig. 3, we found that the chlorine atoms, the bromine atoms, and the hydrogen atoms of the Br_2, SO_2Cl_2, 4-isothiazoline-3-one and 2-methyl-4-isothiazoline -3-one molecules were located in the zone of positive electrostatic potential indicated by the blue color; therefore, these are the most electrophilic sites and these carbon bonds can be considered as possible sites undergoing the nucleophilic attack.

Analysis of the Potential Energy Surface

According to the transition state theory, the transition from reactants (initial state) to products (final state) requires passing through a transition state.

Table 5 shows the energies of the final molecules and the reactants, the energies (E*) of the transition states TS_1, TS_2, TS_3 and TS_4, and the activation energy (E_a) corresponding to the formation of the desired molecules.

It should be noted that the activation energies corresponding to the transition states of reactions 1 and 3 were lower than those corresponding to transition states 2 and 4, which shows that reactions 1 and 3 are more kinetically favored than the reactions 2, 4 (Fig. 4).

The four transition state structures involved in the four reactions and optimized by the DFT B3LYP/6-311G (d, p) are shown in Fig 5.

In Fig. 4, the lengths of the formed C_3-Cl_8 and C_2-Cl_9 (2.508 Å) bonds in the transition state structures TS1 and TS3, and the bond length of C_3-Br (2.800 Å) in the structures of transition states TS2 and TS4 are equal. Therefore, the distribution of total electron density in TS1 and TS3 are similar to that in TS2 and TS4; hence, TS1 and TS3 have similar bonding pattern. The same observation was found for TS2 and TS4 transitions.

NBO Analysis

NBO analysis provides the most possible accurate picture of the "natural Lewis structure", as all orbital details are mathematically chosen to include the highest possible

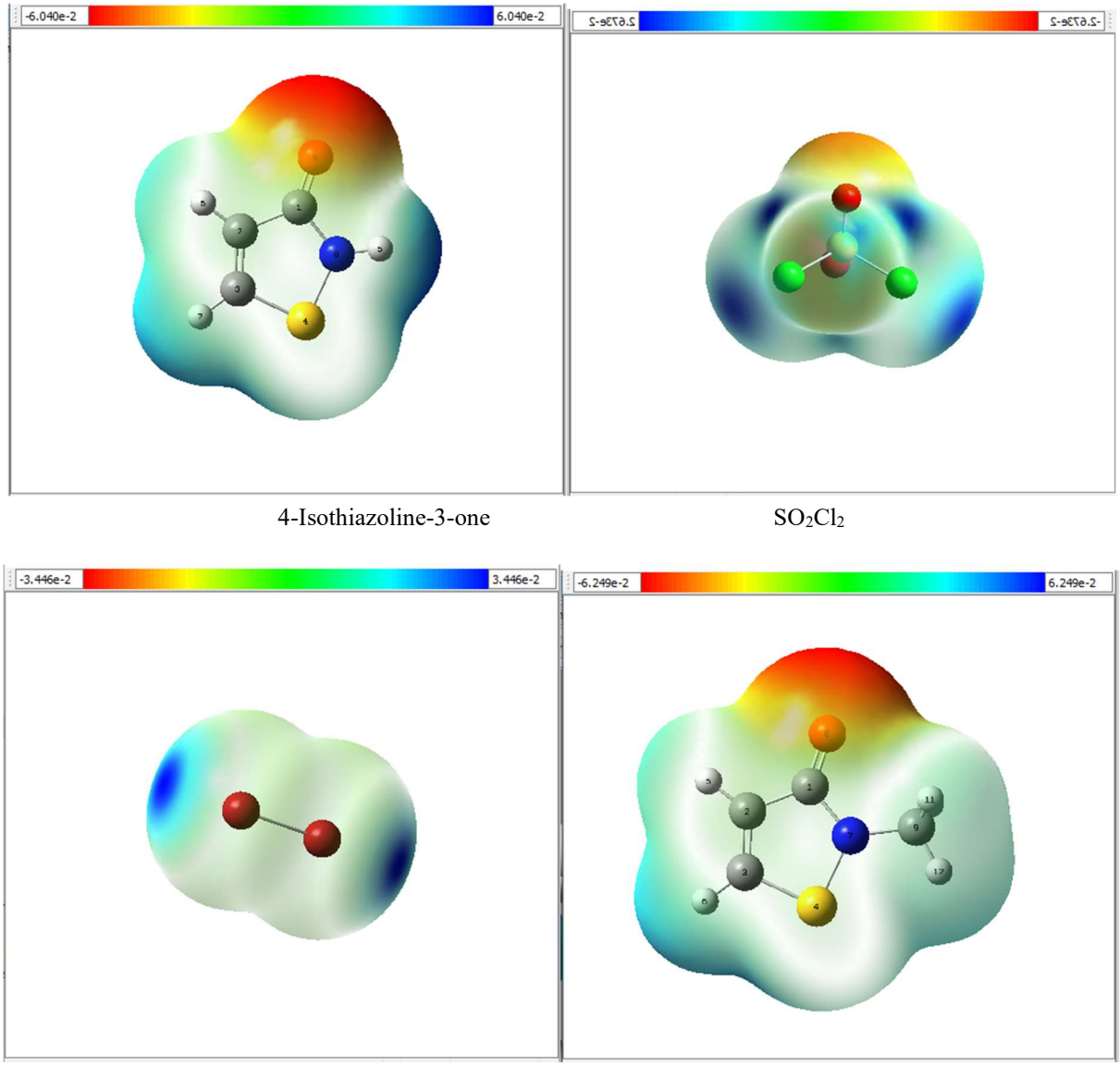

4-Isothiazoline-3-one SO_2Cl_2

Br_2 2-Methyl-4-isothiazoline-3-one

Fig. 3. Mapping of the electrostatic potential around the four molecules.

Table 5. The Energies of the Transition States (E_{TS}), and Activation Energies (E_a) Corresponding to the Formation of the four Molecules Calculated by the DFT Method B3LYP/6-311G(d,p)

	$E_{produits}$ (ua)	$E_{reactants}$ (ua)	E_{TS} (ua)	E_a (kcal mol^{-1})
Reaction 1	-2113.394	-2113.422	-2113.214	112.95
Reaction 2	-5792.649	-5792.64	-5792.59	32
Reaction 3	-2152.715	-2152.742	-2152.537	128.64
Reaction 4	-5831.969	-5831.961	-5831.912	30.74

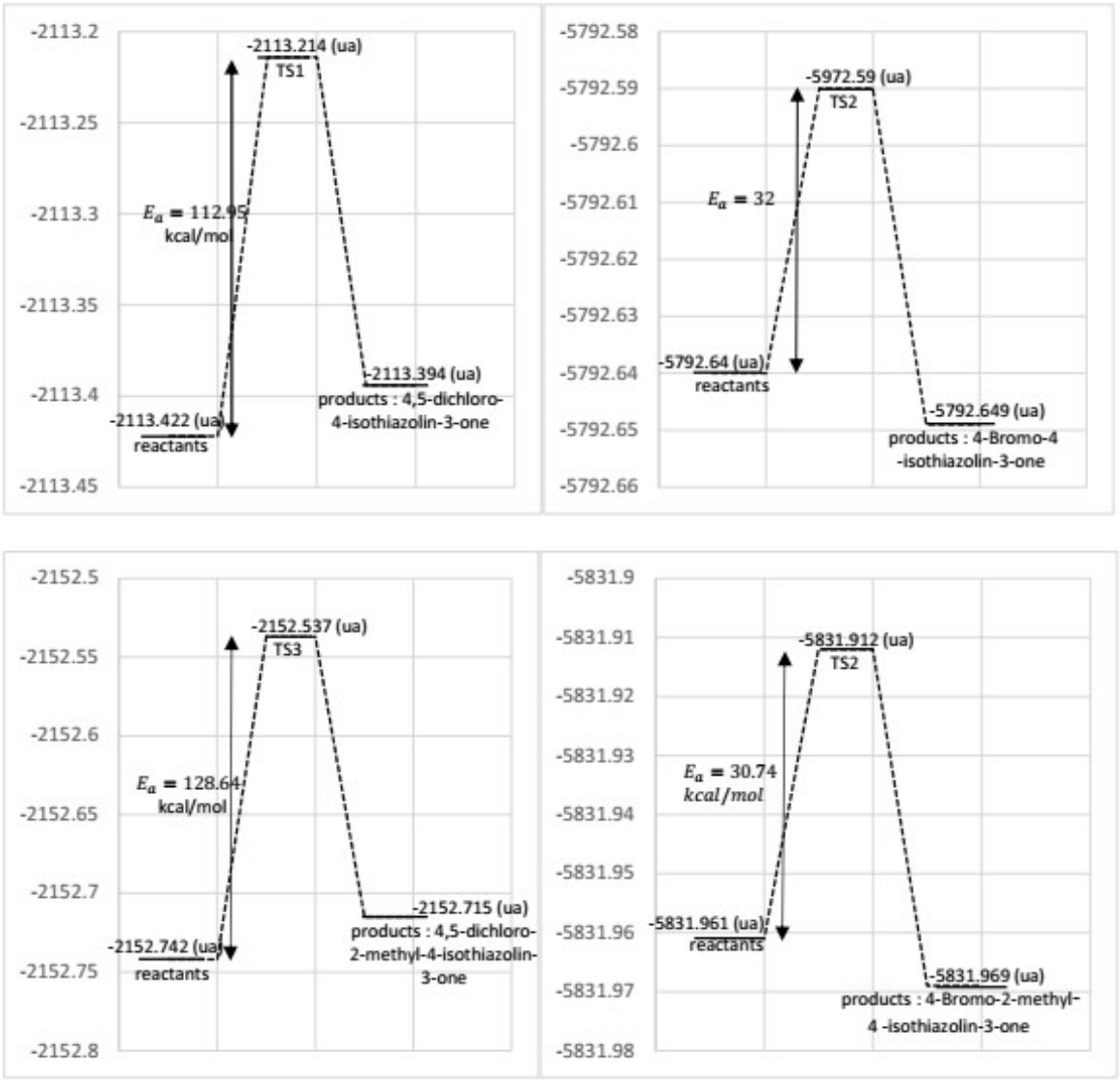

Fig. 4. Hartree energy profile for the 4 reactions studied.

percentage of electron density [38]. In NBO analysis, donor-acceptor (binding-anti-binding) interactions are considered by looking at all possible interactions between "busy" (donor) Lewis-like NBOs and "unbusy" non-Lewis-like NBOs (acceptors). Then, their energies are estimated by second-order perturbation theory [39]. These stabilizing interactions are called "delocalization" corrections of the natural Lewis structure. For each donor, NBO (i) and acceptor NBO (j), the stabilization energy E_2, which is associated with the delocalization i→j, is explicitly estimated by the following equation:

$$E_2 = \Delta E_{ij} = q_i \frac{F(i,j)^2}{E_i - E_j}$$

Here, q_i is the donor orbital occupancy, E_i and E_j are diagonal elements, and F(i,j) is the off-diagonal NBO Fock matrix element.

The occupancy and energies of the i and j orbitals with the ΔE_{ij} of $Lp_{(1)}$, $Lp_{(2)}$, and the bond (σ/π) to antibond (σ*/π*)

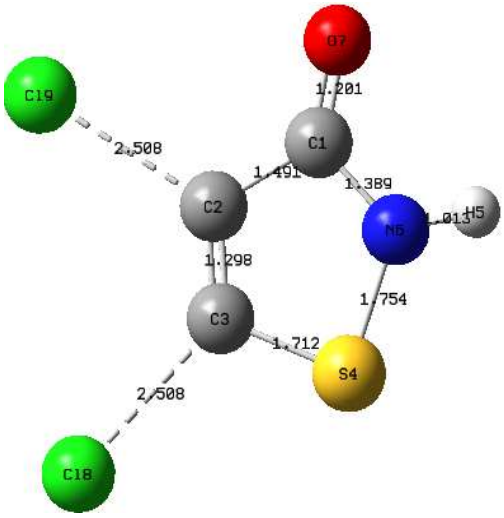

TS1: 4,5-Dichloro-4-isothiazolin-3-one

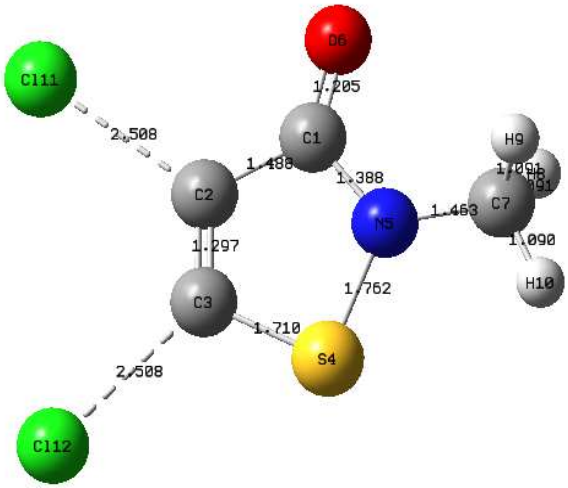

TS3: 4,5-Dichloro-2-methyl-4-isothiazolin-3-one

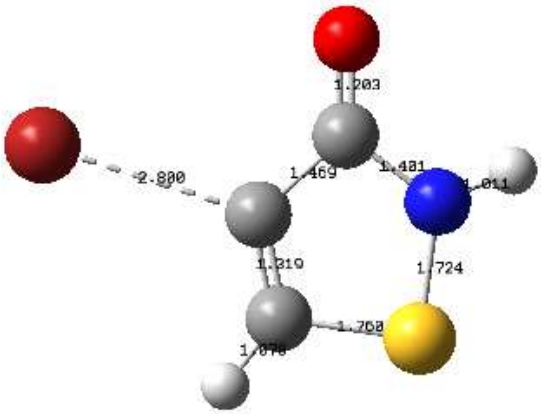

TS2: 4-Bromo-4-isothiazolin-3-one

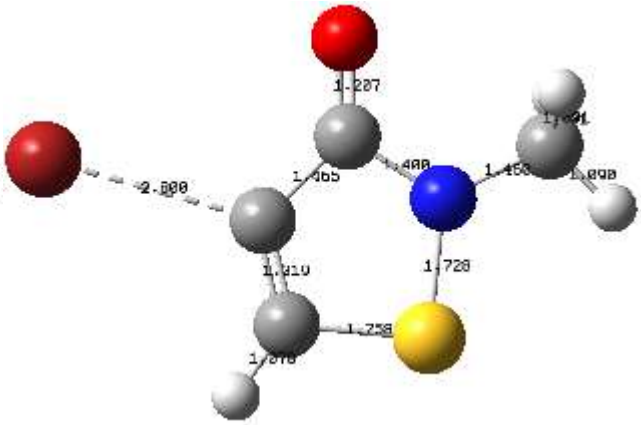

TS4: 4-Bromo-2-methyl-4-isothiazolin-3-one

Fig. 5. Structures of the transition states obtained by DFT B3LYP/6-311G(d,p) involved in the studied reactions.

transitions are given in Table 6. The Lp(1) $N_6 \rightarrow \pi^*$ (C_1-O_7) interaction contributed to a maximum ΔE_{ij} of 51.10 kcal mol^{-1}, 47.75 kcal mol^{-1}, and 48.42 kcal mol^{-1} for 4-bromo-2-methyl-4isothiazolin-3-one, 4-bromo-4-isothiazolin-3-one, and 4,5-dichloro-4-isothiazolin-3-one molecules. For the 4,5-dichloro-2-methyl-4-isothiazolin-3-one molecule, the $N_5 \rightarrow \pi^*$ (C_1-O_6) interaction contributed to a maximum ΔEij of 51.96 kcal mol^{-1}. Binding (σ/π) to antibinding (σ^*/π^*) interactions also contributed significantly to the stability of the structure with a maximum contribution of π (C_2-C_3)/π^* (C_1-O_7) having a ΔEij of 16.47 kcal mol^{-1}, 16.35 kcal mol^{-1}, and 15.01 kcal mol^{-1} for 4-bromo-2-methyl-4-isothiazolin-3-one, 4-bromo-4-isothiazolin-3-one, 4,5-dichloro-4-isothiazolin-3-one molecules. For the 4,5-dichloro-2-methyl-4-isothiazolin-3-one molecule, the π (C_2-C_3)/π^* (C_1-O_7) interaction contributed to a maximum ΔE_{ij} of 15.05 kcal mol^{-1}.

Thermodynamic Parameters

We have calculated the enthalpy H, the entropy S and the free enthalpy G at 25 °C for each molecule (Table 7). The enthalpy H is the summation of the internal energy of a system and the product of its pressure by its volume. Entropy S is characterized by the degree of disorder or unpredictability of the information contained in a system.

We determined that 4-bromo-2-methyl-4-isothiazolin-3-one had a lower G energy; indicating that the 4-bromo-2-methyl-4-isothiazolin-3-one is more thermodynamically stable.

Table 6. Second-order Perturbation Theory Analysis of fock Matrix in NBO Basis

Molecules	Donor	Type	ED/e	Acceptor	Type	ED/e	E(2)	E(j)-E(i)	E(i, j)
4-Bromo-2-methyl-4-isothiazoline-3-one	C_2-C_3	π	1.91205	C_1-O_7	π*	0.36607	16.47	0.34	0.072
	S_4	Lp(2)	1.76327	C_2-C_3	π*	0.28033	22.90	0.27	0.071
	N6	Lp(1)	1.70339	C_1-O_7	π*	0.36607	51.10	0.30	0.113
	O_7	Lp(1)	1.97698	C_1	σ*	0.01746	15.04	1.53	0.136
	O_7	Lp(2)	1.83063	C_1-C_2	σ*	0.08628	19.42	0.66	0.104
	O_7	Lp(2)	1.83063	C_1-N_6	σ*	0.09932	29.12	0.66	0.126
4-Bromo-4-isothiazoline-3-one	C_2-C_3	π	1.91200	C_1-O_7	π*	0.35057	16.35	0.34	0.071
	S_4	Lp(2)	1.76314	C_2-C_3	π*	0.27595	23.07	0.27	0.071
	N_6	Lp(1)	1.74311	C_1-O_7	π*	0.35057	47.75	0.31	0.112
	O_7	Lp(1)	1.97719	C_1	σ*	0.01692	15.50	1.52	0.137
	O_7	Lp(2)	1.82410	C_1-C_2	σ*	0.08962	19.73	0.66	0.104
	O_7	Lp(2)	1.82410	C_1-N_6	σ*	0.09745	29.97	0.64	0.127
4,5-Dichloro-4-isothiazoline-3-one	C_2-C_3	π	1.91016	C_1-O_7	π*	0.34955	15.01	0.35	0.070
	S_4	Lp(2)	1.77677	C_2-C_3	π*	0.35536	22.07	0.25	0.069
	N_6	Lp(1)	1.74832	C_1-O_7	π*	0.3495	48.42	0.31	0.112
	O_7	Lp(2)	1.97734	C_1	σ*	0.01639	15.55	1.53	0.138
	O_7	Lp(2)	1.81557	C_1-C_2	σ*	0.09443	20.93	0.65	0.107
	O_7	Lp(2)	1.81557	C_1-N_6	σ*	0.09571	29.35	0.65	0.126
4,5-Dichloro-2-methyl-4-isothiazoline-3-one	C_2-C_3	π	1.91062	C_1-O_6	π*	0.36524	15.05	0.35	0.070
	S_4	Lp(2)	1.77655	C_2-C_3	π*	0.35779	21.93	0.25	0.069
	N_5	Lp(1)	1.70860	C_1-O_6	π*	0.36524	51.96	0.30	0.114
	O_6	Lp(1)	1.97720	C1	σ*	0.01691	15.03	1.55	0.136
	O_6	Lp(2)	1.82221	C_1-C_2	σ*	0.09137	20.61	0.66	0.106
	O_6	Lp(2)	1.82221	C_1-N_5	σ*	0.09758	28.52	0.66	0.125

Table 7. Thermodynamic Parameters of 4-Bromo-4-isothiazolin-3-one, 4-Bromo-2-methyl-4-isothiazolin-3-one, 4,5-Dichloro-2-methyl-4-isothiazolin-3-one, 4,5-Dichloro-4-isothiazolin-3-one

Molecule	ΔH (kj mol^{-1})	ΔS (kj mol^{-1} K^{-1})	ΔG (kj mol^{-1})
4-Bromo-4-isothiazoline-3-one	-3217.839760	85.423×10^{-3}	-3217.880347
4-Bromo-2-methyl-4-isothiazoline-3-one	-3257.131746	89.149×10^{-3}	-3257.174103
4,5-dichloro-2-methyl-4-isothiazoline-3-one	-1602.831018	93.869×10^{-3}	-1602.875618
4,5-dichloro-4-isothiazoline-3-one	-1563.539854	85.941×10^{-3}	-1563.580688

UV-Vis Spectral Analysis

The electronic absorption spectra of the four molecules in the methanol solution using the TD-DFT method (B3LYP/6-311G(d,p)) were evaluated. The theoretical and experimental absorption wavelengths are compared in Table 8.

As can be seen, all compounds exhibited a common absorption region called the long wavelength region (280-360 nm). The compounds 4,5-dichloro-4-isothiazolin-3-one and 4,5-dichloro-2-methyl-4-isothiazolin-3-one show spectra with its maximum at 280 nm, and with a maximum energy difference of 4.43 eV. On the other hand, the compounds 4-bromo-4-isothiazolin-3-one and 4-Bromo-2-methyl-4-isothiazolin-3-one show strong transitions at 286 nm and 284 nm with a maximum energy differences of 4.34 and4.37 eV; these four compounds showed transitions $\pi \rightarrow \pi^*$.

NMR Spectral Analysis

The NMR spectroscopic tool is a breakthrough method in unraveling the very complex structure of organic molecules. The combined use of experimental and Gaussian computational tools offers a powerful tool to interpret the structure of large molecules.

The optimized structures of the four studied molecules were used to calculate the NMR spectra using the GIAO method. The chemical shifts of the compound are reported in ppm relative to TMS for ^{1}H and ^{13}C (Tables 9 and 10).

According to the ^{13}C NMR spectral analyses, the observed chemical shifts of C_1, C_2, C_3 and C_9 of the 4-bromo-2-methyl-4-isothiazolin-3-one molecule were 165.3, 124.65, 145.16, and 33.6 ppm, respectively. The corresponding chemical shifts for the 4,5-dichloro-2-methyl-4-isothiazolin-3-one molecule were 160.14, 127.33, 151.61, 29.1 ppm, respectively. For the two other molecules, the observed chemical shifts of C_1, C_2 and C_3 were 159.4, 127.01, 154.53 ppm for the molecule 4,5-dichloro-4-isothiazolin-3-one molecule and 163.49, 127.6, 144.09 ppm for the 4-bromo-4-isothiazolin-3-one molecule (Table 9).

For ^{1}H NMR spectra, there were two distinct but very distant peaks for the 4-Bromo-2-methyl-4-isothiazolin-3-one molecule, the first one related to the proton H_7 linked to the C=C double bond coming out at 8.37 ppm and the other corresponded to the CH_3 group which coming out at 3.38 ppm. Similarly, for the 4-bromo-4-isothiazolin-3-one molecule, there were two peaks, one related to hydrogen H_8

Table 8. Theoretical Values of the Electronic Absorption Spectra of the four Studied Molecules

	λ_{max}^{exp} (nm)	$\log(\varepsilon)_{\text{exp}}$	λ_{max}^{cal} (nm)	$\log(\varepsilon)_{\text{cal}}$	E_{cal} (eV)
4,5-Dichloro-4-isothiazolin-3-one			280	6	4.43
4,5-Dichloro-2-methyl-4-isothiazolin-3-one	279	4.09	280	4.5	4.43
4-Bromo-4-isothiazolin-3-one	267	3.88	286	4.2	4.34
4-Bromo-2-methyl-4-isothiazolin-3-one			284	4.2	4.37

Table 9. Isotropic Chemical Shifts δ (ppm) Obtained by GIAO Methods at the Base 6-311G(d,p)

MOLECULE	ATOM	δ_{GIAO}	MOLECULE	ATOM	δ_{GIAO}
4-Bromo-2-methyl-4-isothiazolin-3-one	C_1	165.3	4,5-Dichloro-2-methyl-4-	C_1	160.14
	C_2	124.65	isothiazolin-3-one	C_2	127.33
	C_3	145.16		C_3	151.61
	C_9	33.6		C_9	29.1
4,5-Dichloro-4-isothiazolin-3-one	C_1	159.4	4-Bromo-4-isothiazolin-3-one	C_1	163.49
	C_2	127.01		C_2	127.6
	C_3	154.53		C_3	144.09

Table 10. Isotropic Chemical Shifts δ (ppm) Obtained by GIAO Methods at the Level of the 6-311G Base (d,p) and Experimental ^{1}H NMR [11]

Molecule	ATOM	δ_{GIAO}	δ_{exp}	Molecule	ATOM	δ_{GIAO}	δ_{exp}
4-Bromo-2-methyl-4-	H_7	8.37	8.13	4,5-Dichloro-2-	H_{10}	3.24	3.33
isothiazolin-3-one	H_{10}	3.30	3.38	methyl-4-	H_{11}	3.24	3.33
	H_{11}	3.30	3.38	isothiazolin-3-one	H_{12}	3.24	3.33
	H_{12}	3.30	3.38				
4,5-Dichloro-4-	H_5	4.96	-	4-Bromo-4-	H_5	5.19	-
isothiazolin-3-one				isothiazolin-3-one			

that was at 8.19 ppm, and another peak corresponded to the hydrogen H_5 at 5.19 ppm.

In the case of the two molecules 4,5-dichloro-4-isothiazolin-3-one and 4,5-dichloro-2-methyl-4-isothiazolin-3-one, a single peak of hydrogen H_5 at 4.96 ppm and another peak related to CH_3 carbon at 3.24 ppm were obtained (Table 10).

CONCLUSIONS

The theoretical calculations of the electron density of atoms of the reactants, the electrophilic and nucleophilic character, the local electrophilic and nucleophilic indices, the Fukui indices, the localization of the transition states, and the analysis of the energy surface potential were done using DFT method B3LYP/6-311G(d,p). The following are concluding remarks:

- The difference in overall electrophilicity of the two reactants showed that all the studied reactions had a polar character.
- The most favored interaction took place between the C_2 and C_3 atoms of 4-isothiazolin-3-one and 2-methyl-4-isothiazolin-3-one with the Cl_4 and Cl_5 atoms of sulfuryl chloride and also with the Br atom of dibromine.
- The activation energies corresponding to the transition states of reactions 2 and 3 were lower than those corresponding to transition states 1 and 4.
-

REFERENCES

[1] Castro, M. Á.; Gamito, A. M.; Tangarife-Castaño, V.; Roa-Linares, V.; Miguel del Corral, J. M.; Mesa-Arango, A. C.; Francesch, A. M.; Betancur-Galvis, L.; San Feliciano, A., New 1,4-anthracenedione derivatives with fused heterocyclic rings: synthesis and biological evaluation. *RSC Adv.* **2015**, *5*(2), 1244-1261, DOI: 10.1039/c4ra11726c.

[2] Wang, B. -L.; Zhu, H. -W.; Li, Z. -M.; Wang, L. -Z.; Zhang, X.; Xiong, L. -X.; Song, H. -B., Synthesis, biological evaluation and SAR analysis of novel poly-heterocyclic compounds containing pyridylpyrazole group. *Pest Manage. Sci.* **2017**, *74*(3), 726-736, DOI: 10.1002/ps.4770.

[3] Li, S.; Huang, K.; Cao, B.; Zhang, J.; Wu, W.; Zhang, X., Highly Enantioselective Hydrogenation of β, β-Disubstituted Nitroalkenes. *Angew. Chem. Int. Ed.* **2012**, 51(34), 8573–8576, DOI: 10.1002/anie.201202715.

[4] Zhang, L.; Li, W.; Xiao, T.; Song, Z.; Csuk, R.; Li, S., Design and Discovery of Novel Chiral Antifungal Amides with 2-(2-Oxazolinyl) aniline as a Promising Pharmacophore. *J. Agric. Food. Chem.* **2018**, *66*(34), 8957-8965, DOI: 10.1021/acs.jafc.8b02778.

[5] Wu, Q. -F.; Zhao, B.; Fan, Z. -J.; Zhao, J. -B.; Guo, X. -F.; Yang, D. -Y.; Zhang, N. -L.; Yu, B.; Kalinina, T.; Glukharevab, T., Design, synthesis and fungicidal activity of isothiazole–thiazole derivatives. *RSC Adv.* **2018**, *8*(69), 39593-39601, DOI: 10.1039/c8ra07619g.

[6] Herman, A.; Aerts, O.; de Montjoye, L.; Tromme, I.; Goossens, A.; Baeck, M., Isothiazolinone derivatives and allergic contact dermatitis: a review and update. *J. Eur. Acad. Dermatol. Venereol*. **2018**, *33*(2), 267-276, DOI: 10.1111/jdv.15267.

[7] Schwensen, J. F.; Lundov, M. D.; Bossi, R.; Banerjee, P.; Gimenez-Arnau, E.; Lepoittevin, J. -P.; Lidén, C.; Uter, W.; Yazar, K.; White, I. R.; Johansen, J. D., Methylisothiazolinone and benzisothiazolinone are widely used in paint: a multicentre study of paints from five European countries. *Contact Dermatitis.* **2014**, *72*(3), 127-138, DOI: 10.1111/cod.12322.

[8] Hofmann, M. A.; Giménez-Arnau, A.; Aberer, W.; Bindslev-Jensen, C.; Zuberbier, T., MI (2-methyl-4-isothiazolin-3-one) contained in detergents is not detectable in machine washed textiles. *Clin. Transl. Allergy*. **2018**, *8*(1), DOI: 10.1186/s13601-017-0187-2.

[9] Geier, J.; Lessmann, H.; Schnuch, A.; Uter, W., Recent increase in allergic reactions to methylchloroisothiazolinone/ methylisothiazolinone: is methylisothiazolinone the culprit?. *Contact Dermatitis.* **2012**, *67*(6), 334-341, DOI: 10.1111/j.1600-0536.2012.02157.x.

[10] Oono, H.; Hatai, K., Antifungal Activities of Bronopol and 2-methyl-4-isothiazolin-3-one (MT) against Saprolegnia. *Biocontrol. Sci*. **2007**, *12*(4), 145-148, DOI: 10.4265/bio.12.145.

[11] Lewis, S. N.; Miller, G. A.; Hausman, M.; Szamborski, E. C., Isothiazoles I: 4-isothiazolin-3-ones. A general synthesis from 3,3′-dithiodipropionamides. *J. Heterocycl. Chem.* **1971**, *8*(4), 571-580, DOI: 10.1002/jhet.5570080408.

[12] Frisch, M. J.; Trucks, G. W.; Schlegel, H. B.; Scuseria, G. E.; Robb, M. A.; Cheeseman, J. R.; Scalmani, G.; Barone, V.; Mennucci, B.; Petersson, G. A.; Nakatsuji, H.; Caricato M.; Li X.; Hratchian, H. P.; Izmaylov, A. F.; Bloino, J.; Zheng, G.; Sonnenberg, J. L., Hada, M., Ehara, M., Toyota, K.; Fukuda, R.; Hasegawa, J.; Ishida, M.; Nakajima, T.; Honda, Y.; Kitao, O.; Nakai, H.; Vreven, T.; Montgomery, J. A.; Peralta, J. E.; Ogliaro, F.; Bearpark, M.; Heyd, J. J.; Brothers, E.; Kudin, K. N.; Staroverov, V. N.; Kobayashi, R.; Normand, J.; Raghavachari, K.; Rendell, A.; Burant, J. C.; Iyengar, S. S.; Tomasi, J.; Cossi, M.; Rega, N.; Millam, J. M.; Klene, M.; Knox, J. E.; Cross, J. B.; Bakken, V.; Adamo, C.; Jaramillo, J.; Gomperts, R.; Stratmann, R. E.; Yazyev, O.; Austin, A. J.; Cammi, R.; Pomelli, C.; Ochterski, J. W.; Martin, R. L.; Morokuma, K.; Zakrzewski, V. G.; Voth, G. A.; Salvador, P.; Dannenberg, J. J.; Dapprich, S.; Daniels, A. D.; Farkas, Ö.; Foresman, J. B.; Ortiz, J. V.; Cioslowski, J.; and Fox, D. J., Gaussian, Inc, Wallingford CT., **2009**.

[13] Costa, A. C.; Ondar, G. F.; Versiane, O.; Ramos, J. M.; Santos, T. G.; Martin, A. A.; Raniero, L.; Bussi, G. G. A.; Téllez Soto, C. A., DFT: B3LYP/6-311G(d, p) vibrational analysis of bis (diethyldithiocarbamate) zinc(II) and natural bond orbitals. *Spectrochim. Acta A Mol. Biomol. Spectrosc.* **2013**, *105*, 251-258, DOI: 10.1016/j.saa.2012.11.097.

[14] Costa, A. C.; Ramos, J. M.; Téllez Soto, C. A.; Martin, A. A.; Raniero, L.; Ondar, G. F.; Versiane, O.; Moraes, L. S., Fourier Transform Infrared and Raman spectra, DFT: B3LYP/6-311G(d,p) calculations and structural properties of bis (diethyldithiocarbamate) copper(II). *Spectrochim. Acta A Mol. Biomol. Spectrosc.* **2013**, *105*, 259-266, DOI: 10.1016/j.saa.2012.11.053.

[15] Vektariene, A.; Vektaris, G.; Svoboda, J., A theoretical approach to the nucleophilic behavior of benzofused thieno [3,2-b]furans using DFT and HF based reactivity descriptors. *Arkivoc*. **2009**, (7), 311-329, DOI: 10.3998/ark.5550190.0010.730.

[16] Abraham, C. S.; Muthu, S.; Prasana, J. C.; Armaković, S.; Armaković, S. J.; Rizwana, B. F.; Geoffrey, B.; David R., H. A., Computational evaluation of the reactivity and pharmaceutical potential of an organic amine: A DFT, molecular dynamics simulations and molecular docking approach. *Spectrochim. Acta A Mol. Biomol. Spectrosc.* **2019**, 117188, DOI: 10.1016/j.saa.2019.117188.

[17] Vargas-Sánchez, R. D.; Mendoza-Wilson, A. M.; Balandrán-Quintana, R. R.; Torrescano-Urrutia, G. R.; Sánchez-Escalante, A., Study of the molecular structure and chemical reactivity of pinocembrin by DFT calculations. *Comput. Theor. Chem*. **2015**, *1058*, 21-27, DOI: 10.1016/j.comptc.2015.01.014.

[18] Frau, J.; Glossman-Mitnik, D., Conceptual DFT study of the local chemical reactivity of the dilysyldipyrrolones A and B intermediate melanoidins. *Theor. Chem. Acc.* **2018**, *137*(5), DOI: 10.1007/s00214-018-2244-x.

[19] EL Ouafy, H.; Aamor, M.; Oubenali, M.; Mbarki, M.; EL Haimouti, A.; EL Ouafy, T., Theoretical study of the stability and reactivity of salicylic acid isomers by the DFT method. *Curr. Chem. Lett*. **2022**, *11*(2), 183-190, DOI: 10.5267/j.ccl.2022.3.005.

[20] Pilli, S. R.; Banerjee, T.; Mohanty, K., HOMO-LUMO energy interactions between endocrine disrupting chemicals and ionic liquids using the density functional theory: Evaluation and comparison. *J. Mol. Liq*. **2015**, *207*, 112-124, DOI: 10.1016/ j.molliq.2015.03.019.

[21] Jupp, A. R.; Johnstone, T. C.; Stephan, D. W., The global electrophilicity index as a metric for Lewis acidity. *Dalton Trans.* **2018**, *47*(20), 7029-7035, DOI: 10.1039/c8dt01699b.

[22] Jupp, A. R.; Johnstone, T. C.; Stephan, D. W., Improving the Global Electrophilicity Index (GEI) as a Measure of Lewis Acidity. *Inorg. Chem.* **2018**, *57*(23), 14764-14771, DOI: 10.1021/ acs.inorgchem.8b02517.

[23] Chattaraj, P. K.; Giri, S., Electrophilicity index within a conceptual DFT framework. *Annu. Rep. Prog. Chem., Sect. C: Phys. Chem*. **2009**, *105*, 13-39, DOI: 10.1039/b802832j.

[24] Chattaraj, P. K.; Roy, D. R., Update 1 of: Electrophilicity Index. *Chem. Rev*. **2007**, *107*(9), PR46-PR74, DOI: 10.1021/cr078014b.

[25] Geerlings, P.; De Proft, F.; Langenaeker, W., Conceptual Density Functional Theory. *Chem. Rev*. **2003**, *103*(5), 1793-1874, DOI: 10.1021/cr990029p.

[26] Vessally, E.; Jafari, A. A.; Ahmadi, E., DFT calculations on quetiapine hemifumarate as a pharmaceutical compound for the treatment of schizophrenia. *Iran. Chem. Commun*. **2016**, *4*(1) 123-132.

[27] Domingo, L. R.; Chamorro, E.; Pérez, P., Understanding the Reactivity of Captodative Ethylenes in Polar Cycloaddition Reactions. A Theoretical Study. *J. Org. Chem*. **2008**, *73*(12), 4615-4624, DOI: 10.1021/jo800572a.

[28] Jaramillo, P.; Domingo, L. R.; Chamorro, E.; Pérez, P., A further exploration of a nucleophilicity index based on the gas-phase ionization potentials. *Theochem*. **2008**, *865*(1-3), 68-72, DOI: 10.1016/j.theochem.2008.06.02.

[29] Domingo, L. R.; Pérez, P., Global and local reactivity indices for electrophilic/nucleophilic free radicals. *Org. Biomol. Chem*. **2013**, *11*(26), 4350, DOI: 10.1039/c3ob40337h.

[30] Domingo, L.; Ríos-Gutiérrez, M.; Pérez, P., Applications of the Conceptual Density Functional Theory Indices to Organic Chemistry Reactivity. *Molecules.* **2016**, *21*(6), 748, DOI: 10.3390/molecules21060748.

[31] Domingo, L. R.; Chamorro, E.; Pérez, P., Understanding the Reactivity of Captodative Ethylenes in Polar Cycloaddition Reactions. A Theoretical Study. *J. Org. Chem*. **2008**, *73*(12), 4615-4624, DOI: 10.1021/jo800572a.

[32] Domingo, L. R.; Pérez, P., The nucleophilicity N index in organic chemistry, *Org. Biomol. Chem*. **2011**, *9*(20), 7168, DOI: 10.1021/jo800572a.

[33] Pérez, P.; Toro-Labbé, A.; Aizman, A.; Contreras, R., Comparison between Experimental and Theoretical Scales of Electrophilicity in Benzhydryl Cations. *J. Org. Chem*. **2002**, *67*(14), 4747-4752, DOI: 10.1021/jo020255q.

[34] Contreras, R.; Andres, J.; Safont, V. S.; Campodonico, P.; Santos, J. G., A Theoretical Study on the Relationship between Nucleophilicity and Ionization Potentials in Solution Phase. *J. Phys. Chem*. **2003**, *107*(29), 5588-5593, DOI: 10.1021/jp0302865.

[35] Yang, W.; Mortier, W. J., The use of global and local molecular parameters for the analysis of the gas-phase basicity of amines. *J. Am. Chem. Soc*. **1986**, *108*(19), 5708-5711, DOI: 10.1021/ja00279a008.

[36] Cankaya, N.; Tanış, E.; Gülbaş, H. E.: Bulut, N., A new synthesis of limonene copolymer: experimental and theoretical analysis. *Polymer Bulletin*. **2018**, *76*(3), 3297-3327, DOI: 10.1007/s00289-018-2543-3.

[37] Han, J.; Lee, H.; Tao, F. -M., Molecular Structures and Properties of the Complete Series of Bromophenols: Density Functional Theory Calculations. *J. Phys. Chem. A.* **2005**, *109*(23), 5186-5192, DOI: 10.1021/jp0515378.

[38] Sebastian, S.; Sundaraganesan, N., The spectroscopic (FT-IR, FT-IR gas phase, FT-Raman and UV) and NBO analysis of 4-Hydroxypiperidine by density

functional method. *Spectrochim. Acta A Mol. Biomol. Spectrosc. SPECTROCHIM ACTA A.* **2010**, *75*(3), DOI: 10.1016/j.saa.2009.11.030.

[39] Villemin, D.; Charif, I. E.; Mekelleche, S. M.; Bar, N., Natural Bond Orbital Analysis of Cyclic and Acyclic "C-H" Acids. *Eur. Chem. Bull.* **2016**, *5*(7), 274-279, DOI: 10.17628/ECB.2016.5.274.